ISBN: 978-3-95450-168-7 doi:10.18429/JACoW-IPAC2015-MOPMA001

COMPARISON OF MEASUREMENTS AND SIMULATIONS OF SINGLE BUNCH INSTABILITIES AT DIAMOND

M. Atay[2], R.T. Fielder[1], I. Martin[1] and R. Bartolini[1,2]
[1]Diamond Light Source, Oxfordshire, UK
[2]John Adams Institute, University of Oxford, Oxfordshire, UK

Abstract

The single bunch dynamics in the Diamond storage ring has been analysed with a multiparticle tracking code and compared with the results of a wealth of diagnostics under development at Diamond. The interplay of various wakefield sources has been studied and it has been found that the THz spectrum can be reproduced in many cases with simple impedance models, both below and above the bursting threshold.

INTRODUCTION

The study of single bunch instabilities in modern light sources has been fostered by the user requirements to operate the storage rings with short electron bunches for the generation of short X-ray pulses or coherent THz radiation. Diamond has developed a number of low-alpha optics tailored to different users' requirements [1] attempting to optimize either the short X-ray pulse operation ($\alpha \sim 10^{-5}$) or the coherent THz radiation ($\alpha \sim 4\cdot10^{-6}$) [2]. This process has also stimulated the development of advanced THz diagnostics and data collection techniques described in a companion paper [3]. Numerous measurements has been carried out in the past to investigate the rich phenomenology associated to the single bunch instabilities, under different machine conditions, both below and above the instability thresholds. At the same time we have developed a macroparticle tracking code in order to gain a better insight in the mechanism driving the instabilities with the aim of reproducing the complex dynamics and guide further optimisation of the machine performance. The tracking code has been specifically tailored to replicate the data available from our diagnostics, such as THz spectrograms, streak camera images, BPM data and FTIR spectra. We present the first preliminary results of the comparisons between the measurements and tracking simulations and address the issues met.

TRACKING CODE

The beam dynamics in presence of wakefields can be described with various numerical techniques [4]. We have chosen to develop a multiparticle tracking code to study the single bunch dynamics with the influence of wakefields in 6-dimensional phase space, extending the capabilities of the code "sbtrack" [5]. While the original code was written in C, it was later translated to MATLAB to exploit its graphical capability. A number of wakefields have been implemented: most notably resistive wall (RW), coherent synchrotron radiation (CSR), shielded CSR [6] and any number of broad band resonators (BBR). The last option allows the implementation of the wakefields as computed from CST Microwave studio [7] or Gdfidl [8] by fitting a number of BBR models to the most prominent modes.

The code integrates the 6D equations of motion of the electron in the presence of the RF potential, synchrotron radiation damping and diffusion. The link to the full accelerator tracking with AT is under development, although the first tests resulted in prohibitively long computation times. The different impedance models used and the construction of the overall impedance model are described in more details below.

The output of the tracking code is the phase space evolution of the 6D macroparticle distribution on a turn by turn basis This is post-processed to extract all the relevant data that can be measured in the machine, such as tuneshifts, rise time or damping time of the instabilities, turn-by-turn and orbit data, THz emission power, spectrograms and streak camera images. All those quantities can be computed and measured as a function of the single bunch current and the various different machine parameters.

BUILDING THE IMPEDANCE MODEL

The code uses several different types of wakefields. The wake function of the broad band resonator (BBR) model is given by [4]

$$W(z) = 2\alpha R_s e^{\alpha z/c}\left(\cos\frac{\bar{\omega}z}{c} + \frac{\alpha}{\bar{\omega}}\sin\frac{\bar{\omega}z}{c}\right) \quad (1)$$

where $\alpha = \omega_R/2Q$, $\bar{\omega} = \sqrt{\omega_R^2 - \alpha^2}$, Q is a quality factor, ω_R is a resonance frequency and R_s is a shunt impedance. The CSR model is described in [6] and the shielding is taken into account as follows:

$$W(z) = -\frac{2\pi R}{4\pi\varepsilon_0}eN_e\left(\int_0^\infty \frac{2}{(3R^2)^{1/3}}\frac{d\rho(z-z')}{dz}\frac{dz'}{z'^{1/3}} - \right. \\ \left. -\frac{1}{2h^2}\int_{-\infty}^{\infty}\rho(z-z')dz' G_2\left[\frac{1}{2h}\left(\frac{R}{h}\right)^{1/2}z'\right]dz'\right) \quad (2)$$

where 2h is the gap between the shielding plates and R is the bending magnet radius. Purely resistive and purely inductive impedances have also been implemented to be able to accurately characterize the impedance of the storage ring, according to the respective wake functions:

ISBN: 978-3-95450-168-7 doi:10.18429/JACoW-IPAC2015-MOPMA001

$$W_R(z) = -\frac{Rc}{\sigma_{z0}}\delta(z)$$

$$W_L(z) = -\frac{L}{\sigma_{z0}}\frac{\partial\delta(z)}{\partial z}$$

where σ_{z0} is the bunch length, c is the velocity of light, R is the resistive impedance, and L is the inductive impedance.

It should be stressed that a good numerical accuracy is obtained by tracking 1M macroparticles for a number of turns sufficient for the instability to develop and reach to an equilibrium or a stationary behaviour. The code uses the numerical solution of the Haissinki equation as a starting point for the electron bunch distribution. In many cases this is necessary to reduce the perturbation arising from an initial beam distribution that is not matched to the RF bucket and its potential well distortion.

The numerical impedance model is built by using the shielded CSR and the BBR impedance where ω_R and Q are used as fit parameters to match the current dependent bunch length and the centroid shift with current to the experimental data. We found that using either the shielded CSR impedance or a single BBR model is not sufficient to reproduce the data; the combination of the two is essential. While an additional inductive impedance is required to produce a better match for longer bunches, in line with previous investigation [5], it was not used in this comparison.

The impedance model obtained in this way is used to compute the THz emission from the bunch. The radiation emitted by the macroparticle particle is computed from the relation

$$P(\omega) = P_{sp}(\omega)[N_e + N_e^2 \mid f(\omega) \mid] \qquad (3)$$

where N_e is the number of electrons in the bunch and $f(\omega)$ is the bunch form factor. The single particle emission is approximated to $P_{sp}(\omega) \sim \omega^{1/3}$ as coherence effects occur well within the limit of validity of this approximation for the bending magnet radiation spectrum. The coherent part of the emission is the term proportional to the form factor. The power increase is described by the CSR gain defined as $N_e|f(\omega)|$.

The power emitted by the bunch at each turn is frequency selected to match the bandwidth of the Schottky diode used. In this way the code simulates the time variation of the signals measured at our detectors. These time series are Fourier analysed and the spectrogram obtained is then compared with the measured one to validate the impedance model.

COMPARISON MEASUREMENTS AND SIMULATIONS

A large number of machine conditions have been investigated both experimentally and numerically, and a full extensive comparison is still under way. Great care has been taken in providing a full set of measurements for each machine condition, including bunch lengthening curves and THz spectrograms. More recently these experimental data can be acquired synchronously [3].

We report here two examples of comparison of measured and simulated spectrograms. The data are taken for $\alpha = -10^{-5}$, RF voltage V_{RF} = 3.4 MV, and for $\alpha = -1.4\cdot10^{-5}$, RF voltage V_{RF} = 4 MV, respectively. The analysis of the bunch lengthening curve suggests a BBR impedance with resonant frequency of $\nu = \omega/2\pi$ = 41.4 GHz and a shunt resistance R_s = 36 kΩ. The comparison shows a good qualitative agreement between the measured (Fig. 1) and simulated (Fig. 2) spectrograms. The detector bandwidth is 60-90 GHz. In Fig. 2 we were able to reproduce the sharp transition in the current-frequency pattern of the THz pulses occurring at ~60 μA. At this current threshold, the frequencies appearing the spectrogram correspond to the second harmonics of the synchrotron frequency (2*677 Hz) and its multiples, indicating that the bunch is undergoing a strong quadrupole oscillation in the longitudinal phase space.

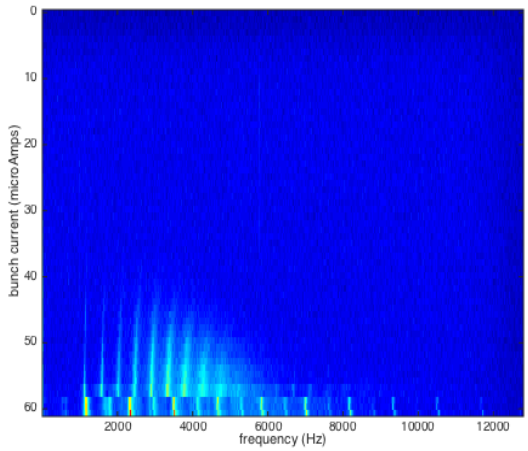

Figure 1: Measured spectrogram for $\alpha = -10^{-5}$, RF voltage V_{RF} = 3.4 MV.

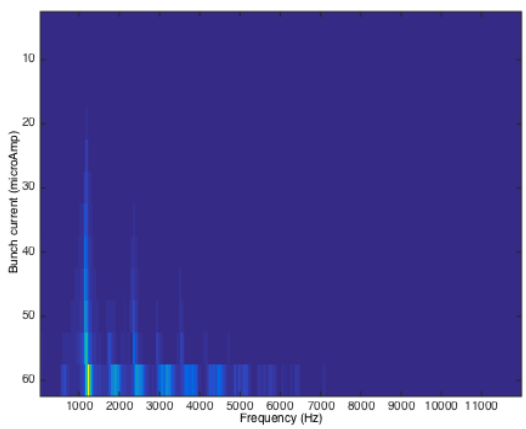

Figure 2: Simulated spectrogram for the same conditions of Fig. 1.

ISBN: 978-3-95450-168-7 doi:10.18429/JACoW-IPAC2015-MOPMA001

Furthermore we observed that the emission of a THz burst is accompanied by an energy loss that induces transverse oscillation of the beam due to dispersion. The Fourier transform of the bunch oscillations can be detected at the BPM and does show the presence of the synchrotron frequency during bursting [3], while this frequency does not appear in the THz spectrogram that is sensitive only to bunch length oscillations.

The second example is reported in Figs. 3-4. The same broad band impedance was used in the simulation in this case. Again, the general characteristics of the THz spectrogram are well reproduced, with a main series of frequencies alternating with weaker ones.

In general, the observed time and frequency patterns of the THz emission have a very rich phenomenology and depend strongly on the machine parameters and the current. Transitions between regular emission patterns and chaotic bursting are evident in many cases, and are abruptly triggered by tiny variations in current. We have observed quite a sharp difference in the behaviour of the bunch dynamics and the corresponding THz spectrograms in comparing the low alpha operation with positive and negative alpha.

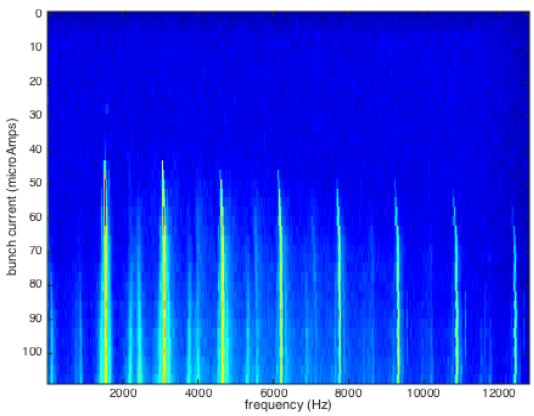

Figure 3: Measured spectrogram for $\alpha = -1.4 \cdot 10^{-5}$, RF voltage $V_{RF} = 4$ MV.

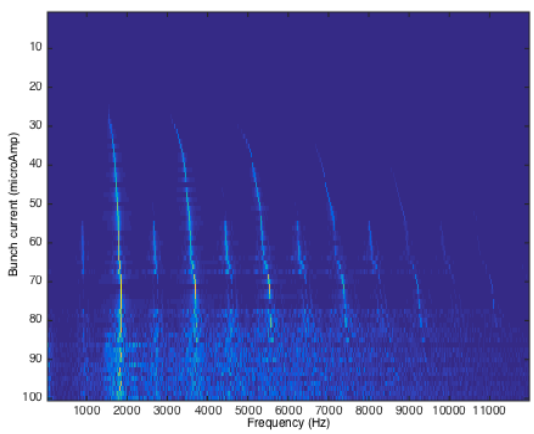

Figure 4: Simulated spectrogram the same conditions as in Fig. 3.

The analysis of the evolution of the bunch distribution shows that the instability for positive alpha is triggered by the development of microbunch structures in the bunch, while the negative alpha case seems to develop a strongly skewed longitudinal profile without any microbunching. It is not clear yet if this is a general behaviour of the two configurations and more analysis is necessary to understand which modes are excited in the bunch. The skewness of the distribution is sufficient to generate coherent THz emission at wavelengths as low as 200 um (50 cm^{-1}). This is shown in Fig. 5 where the CSR gain computed numerically is reported as a function of the wavenumber. These results are in line with the data obtained from the FTIR at the bending magnet beamline B22 [9].

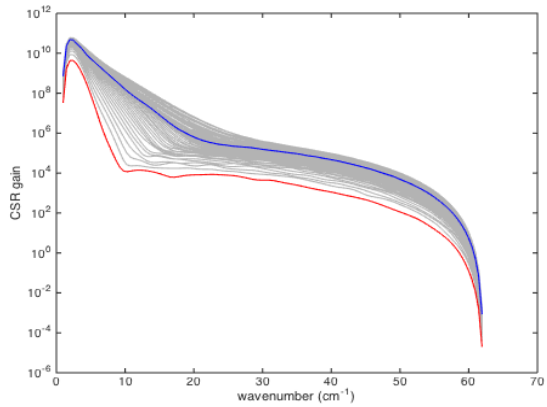

Figure 5: Simulated CSR gain for increasing current in the machine conditions of Fig. 3: (red) is the zero current limit, (blue) is the current threshold for bursting.

CONCLUSION

Single bunch instabilities are under investigation at the Diamond Light Source in order to understand the machine impedance and devise better operational configurations for X-ray short pulses users and the coherent THz users. The development of advanced diagnostics and tracking simulation codes provides two powerful complementary tools to gain insight on the complex dynamics, to understand what triggers the instability and describe the beam dynamics beyond threshold.

REFERENCES

[1] I.P.S. Martin et al., PRSTAB **14**, 040705 (2011).
[2] I.P.S. Martin et al., MOPEA070, Proc. of IPAC'13, Shanghai, China (2013); http://www.JACoW.org
[3] I.P.S. Martin et al., MOPMA003, Proc. of IPAC'15, Richmond, VA, USA (2015); http://www.JACoW.org
[4] A.W. Chao, *Physics of Collective Beam Instabilities in High Energy Accelerators*, (New York: John Wiley & Sons, 1993).
[5] R. Nagaoka et al., FR5RFP046, Proc. of PAC'09, Vancouver, BC, Canada (2009); http://www.JACoW.org
[6] J.B. Murphy et al., Part. Accel. **57**, 9 (1997).

ISBN: 978-3-95450-168-7 doi:10.18429/JACoW-IPAC2015-MOPMA001

[7] CST Microwave Studio, CST UK Limited.
[8] W. Bruns, "The GdfidL Electromagnetic Field Simulator", http://www.gdfidl.de
[9] R. Bartolini, slides presented at the TWIICE workshop, SOLEIL, Paris, January 2014.